Characterization of the Gel Phases of $AlPO_4$-11 Molecular Sieve Synthesis by Solid-state NMR

Yining Huang,* Roger Richer, and Christopher W. Kirby

Contribution from Department of Chemistry, The University of Western Ontario, London, Ontario, Canada N6A 5B7

Received: August 14, 2002; In Final Form: December 3, 2002

We have used several solid-state NMR techniques in conjunction with powder X-ray diffraction (XRD) and FT-Raman spectroscopy to characterize the structures of the intermediate phases of $AlPO_4$-11 molecular sieve synthesis. The evolution of the gel phases as a function of crystallization time was followed by ^{31}P and ^{27}Al magic angle spinning (MAS) NMR to obtain information on the local environments of Al and P atoms and by powder XRD to detect the long range ordering of the gel samples. We have utilized ^{27}Al triple-quantum MAS (3QMAS) to gain additional resolution for monitoring the incorporation of different Al sites into the framework during the crystallization. $^{27}Al/^{31}P$ double resonance techniques such as cross polarization (CP), transfer of populations by double-resonance, and rotational echo double-resonance have been utilized to select the $^{31}P-O-^{27}Al$ bonding connectivities within the gel phases. The $^1H \rightarrow {}^{31}P$ CP enables differentiation of the phosphorus sites in different phases coexisting in the same solid sample. FT-Raman spectroscopy also provides insight into the interactions between organic template and inorganic gel species as well as the evaluation of the pore system. The present work clearly demonstrates that the dipolar-coupling based double-resonance techniques can provide important connectivity information regarding the structures of the gels, which are not readily available from simple MAS experiments.

Introduction

Microporous materials (often referred to as molecular sieves) are a class of inorganic solids with regular pores and cavities in the size range of 5−20 Å. Zeolites that are aluminosilicates represent the most well-known family of such materials. They are extensively used in industry as catalysts, ion-exchangers, and sorbents. Zeolites have been established industrial materials since the 1960s, but in recent years, there has been growing interest in a new class of molecular sieves, namely, the aluminophosphates ($AlPO_4$s)[1]. Some of these materials have the framework topologies of known zeolites, but many have novel structures. These $AlPO_4$-based materials exhibit distinct molecular sieving characteristics and can be made catalytically active by introducing other elements (such as Si) into the framework.

Because of a wide range of practical applications, the synthesis of new microporous materials is one of the major activities in materials science (see ref 2 for some reviews on molecular sieve synthesis). However, despite much data having been compiled on the synthesis conditions, the understanding of the fundamental processes occurring during crystallization on a molecular level is still incomplete. $AlPO_4$'s are usually prepared by hydrothermal synthesis. The processes involve the formation of intermediate gels in the early stages of the reaction. The gel phases eventually transform into crystalline molecular sieves. However, the mechanisms by which the intermediate gel phases transform to the crystalline molecular sieves are particularly poorly understood. This problem arises from the fact that the structural properties of the intermediate phases are usually poorly characterized because of their amorphous nature. Zeolite synthesis has been extensively studied by ^{29}Si and ^{27}Al NMR[3]. Although ^{31}P and ^{27}Al solid-state NMR has been widely used to characterize the framework structures of $AlPO_4$-based molecular sieves,[4] there are far fewer NMR studies dealing with the crystallization of $AlPO_4$'s. In the past, ^{31}P and ^{27}Al magic angle spinning (MAS) methods were mainly utilized to examine the gel phases (although $^1H \rightarrow {}^{31}P$ cross polarization was also sometimes employed). MAS approach is extremely useful in providing information on the local environments of P and Al atoms. However, simple MAS does not directly yield the $^{27}Al-O-^{31}P$ connectivity in the gel phases. Recently, we have shown that $^{27}Al/^{31}P$ cross polarization (CP) can be used to map out the $^{27}Al-O-^{31}P$ connectivity in the intermediate gel phases of VPI-5 synthesis.[5] One of the aims in the present study is to further explore the feasibility of utilizing $^{27}Al/^{31}P$ heteronuclear dipolar coupling based double-resonance solid-state NMR experiments such as CP,[6] transfer of populations in double-resonance (TRAPDOR),[7] and rotational-echo double-resonance (REDOR)[8] to select the $^{27}Al-O-^{31}P$ connectivity in the gel phases.

In this work, we have examined the intermediate gel phases formed during the synthesis of microporous $AlPO_4$-11 molecular sieves by NMR in conjunction with powder X-ray diffraction (XRD) and FT-Raman spectroscopy. In particular, we have utilized a wide range of solid-state NMR techniques including ^{31}P and ^{27}Al MAS NMR, $^{27}Al \rightarrow {}^{31}P$ CP, ^{31}P $\{^{27}Al\}$ TRAPDOR, ^{31}P $\{^{27}Al\}$ REDOR, ^{27}Al multiple quantum magic angle spinning (MQMAS),[9] and $^1H \rightarrow {}^{31}P$ CP NMR techniques to solve particular structural problems wherever they are applicable.

$AlPO_4$-11 was first synthesized by Union Carbide.[10] This sieve has AEL structure, which contains a unidimensional channel system with 10-membered ring noncircular pores (6.7 × 4.4 Å).[11] There are several reports on the synthesis of $AlPO_4$-

* To whom correspondence should be addressed. E-mail: yhuang@uwo.ca.

10.1021/jp021878a CCC: $25.00
Published on Web 01/21/2003

11 with emphasis on the gel chemistry,[12] but none of them involved using NMR to systematically characterize the intermediate gel phases. The crystalline $AlPO_4$-11 molecular sieve itself has been the subject of several solid-state NMR studies. Most of these studies involved using ^{27}Al double rotation (DOR)[13] and ^{27}Al MQMAS[14] to resolve five crystallographically nonequivalent Al sites in its calcined and rehydrated phase, which has lower symmetry (space group $Pna2_1$)[15] than the as-made phase (space group $Ima2$).[11]

Experimental Section

The aluminum and phosphorus sources were $Al(OH)_3$ (50% Al_2O_3) and 85% H_3PO_4, respectively. Di-*n*-propylamine (DPA) was used as structural directing agent. All of the chemicals were purchased from Aldrich Chemical Co. The crystalline $AlPO_4$-11 and corresponding gel phases were prepared with gel composition $1.0Al_2O_3$:$1.0P_2O_3$:$1.0Pr_2NH$:$40H_2O$ according to Tapp et al.[12a] A typical procedure for the preparation of the gel is as follows: 23.4 g of aluminum hydroxide was stirred with 75 g of water, and then 28.2 g of 85% phosphoric acid was added. The mixture was well stirred for 1 h. Then 12.4 g of DPA was added dropwise with continuous stirring. The gel was further stirred for 2 h at room temperature for homogeneity. The reaction mixture (the initial gel without heating) was charged into several autoclaves and first aged at 90 °C for 24 h. The crystallization was then carried out at 200 °C. The autoclaves were quenched at specific times in an ice bath, and the liquid phase of each autoclave was separated from the solid phase by centrifugation. The solid materials were carefully dried in air at room temperature. All of the solid gel samples were kept in tightly sealed glass vials once dried. They were periodically checked by ^{31}P and ^{27}Al MAS NMR and powder XRD, and there was no change in either the NMR spectra or XRD patterns during the course of the study. For selected samples, we examined the same gel samples with different water contents (i.e., completely dried and relatively wet samples). Their NMR results were identical.

All of the NMR experiments were performed on a Varian/Chemagnetics Infinityplus 400 WB spectrometer equipped with three rf channels. At the field strength of 9.4 T, the resonance frequencies are 399.491, 161.968, and 104.293 MHz for ^1H, ^{31}P, and ^{27}Al, respectively. The magic angle was set using the ^{79}Br resonance of KBr. The ^{31}P and ^{27}Al shifts were referenced to 85% H_3PO_4 and 1 M $Al(NO_3)_3$ aqueous solution, respectively. Depending on the requirements of the individual experiment, two NMR probes (a Varian/Chemagnetics 7.5-mm triple tuned T3 MAS probe and a 3.2-mm H/X double tuned MAS probe) were used. The standard MAS NMR spectra were obtained by using the 7.5-mm probe with a spinning speed in the range 5−7 kHz. For ^{31}P MAS experiments, a pulse length of 3 μs (30° pulse) was typically used and the recycle delay was 60 s. The rf field strength for ^1H decoupling was about 50 kHz. The ^{27}Al MAS spectra were acquired using short excitation pulses (less than 1 μs, corresponding to magnetization tip angles of less than 10°) and a pulse delay of 200 ms.

The 7.5-mm probe was used for $^{27}Al \rightarrow {}^{31}P$ CP experiments. Because ^{27}Al ($I = 5/2$) is a quadrupolar nucleus, the cross polarization was carried out in the sudden passage regime (weak rf spin-locking field and fast sample spinning).[16] The modified Hartmann−Hahn matching condition[16] is

$$\gamma_p B_{1,P} = 3\gamma_{Al} B_{1,Al} \pm n\nu_r \qquad n = 1 \text{ or } 2$$

The strength of the ^{27}Al spin-locking field is typically 15−21 kHz, corresponding to the ^{27}Al 90° pulse lengths between 17 and 12 μs measured for the central transition. The spinning rate used for experiments ranged from 5.5 to 7 kHz. The $^{27}Al \rightarrow {}^{31}P$ CP experimental optimization was carried out using crystalline as-made $AlPO_4$-11. Although the optimal contact time for $^{27}Al \rightarrow {}^{31}P$ CP was about 2 ms, a shorter contact time of 0.8 or 1 ms was used to ensure that the CP experiments probe direct Al−O−P linkages. The pulse delay was 100 ms. The two-dimensional $^{27}Al \rightarrow {}^{31}P$ CP (HETCOR) was performed using the approach described by Fyfe et al.[6b] The TPPI method was used in the 2D data acquisition and processing.

The TRAPDOR experiment is specifically designed to probe the heteronuclear dipolar interactions involving, at least, one quadrupolar nucleus (irradiated spin).[7] The TRAPDOR experiment consists of two separate experiments.[7b] The first is a control experiment, in which a rotor synchronized ^{31}P spin−echo sequence ($90°-n\tau_r-180°-n\tau_r$) is applied with τ_r being one rotor period. The second (TRAPDOR) experiment is the same spin−echo as the first except that during the first half of the echo ($n\tau_r$) on the observed ^{31}P spins the ^{27}Al spins are continuously irradiated. The continuous high-power rf irradiation of the ^{27}Al spins under MAS conditions affects the echo intensity of ^{31}P spins via dipolar coupling. The TRAPDOR difference spectrum (ΔS) is obtained by subtracting the TRAPDOR spectrum (S) from the control spectrum (S_0) and indicates dipolar coupling. The REDOR experiment[8] is also a rotor synchronized double resonance MAS technique, and its principle is similar to that of TRAPDOR. This technique involves two experiments with the first one being normal spin−echo experiment on ^{31}P (observing nucleus). In the second (REDOR) experiment, during the spin−echo on ^{31}P, a number of 180° pulses are applied to ^{27}Al (dephasing nucleus) rather than continuous irradiation in TRAPDOR. The echo intensity of REDOR experiments will decrease because of a nonzero average of dipolar coupling compared to the normal echo without 180° dephasing pulses. Similar to TRAPDOR, the REDOR difference spectrum provides the measure of dipolar coupling. The ^{31}P $\{^{27}Al\}$ TRAPDOR experiments[6b,7b−c] were carried out using a 8-μs 90° pulse for ^{31}P, a rf field strength of 45 kHz for ^{27}Al irradiation. The ^{31}P $\{^{27}Al\}$ REDOR experiments were conducted using the standard pulse sequence described in refs 6b and 8b. A 8-μs 90° pulse was also used for ^{31}P and ^{27}Al 180° dephasing pulse length was typically 18 μs. In both TRAPDOR and REDOR experiments, the samples were spun at 6 kHz ± 3 Hz, and a recycle delay of 90 s was necessary to allow full recovery of ^{31}P equilibrium magnetization.

The ^{27}Al triple quantum (3Q) MAS experiments were performed using the 3.2-mm probe capable of producing a rf field of 200 kHz. The 3QMAS spectra were obtained by utilization of a three-pulse, *z*-filer sequence.[17] The rf strengths of the first two hard pulses and the third soft pulse were individually optimized, and the optimized pulse lengths were typically 2.5, 0.85, and 11.5 μs for the three consecutive pulses.

For $^1H \rightarrow {}^{31}P$ cross polarization experiments, the 7.5-mm probe was employed. The ^1H 90° pulse length was 6 μs, and the Hartmann−Hahn condition was determined using $(NH_4)H_2PO_4$. A repetition time of 5 s was used.

The powder XRD patterns of the gels were recorded on a Rigaku diffractometer using Co Kα radiation (a wavelength of 1.7902 Å).

Raman spectra were recorded on a Bruker RFS 100/S FT-Raman spectrometer equipped with an Nd^{3+}:YAG laser operating at 1064.1 nm and a liquid nitrogen cooled Ge detector. The

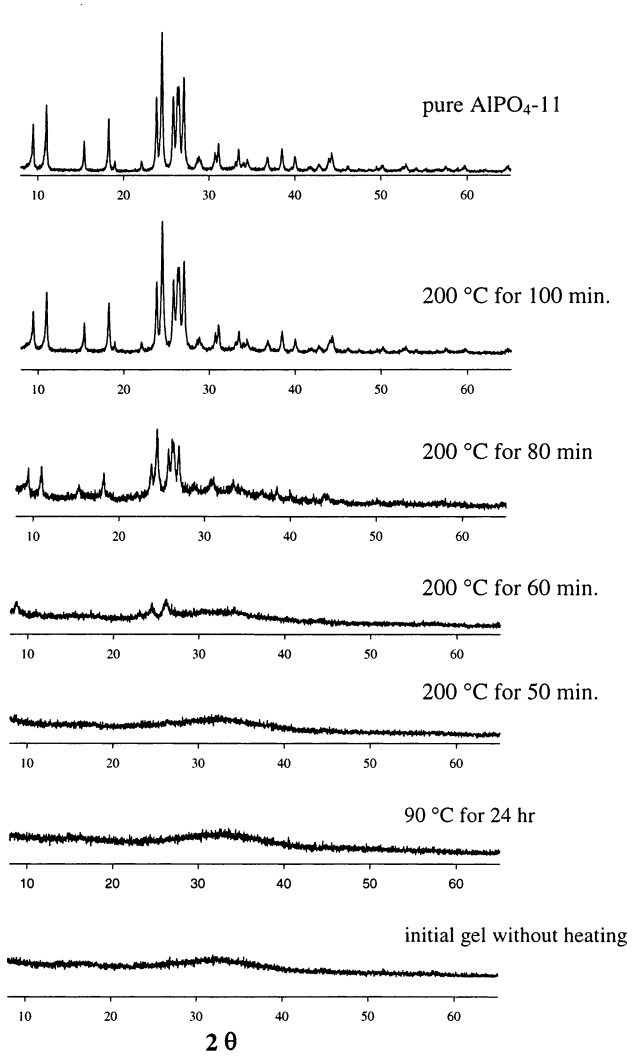

Figure 1. Powder XRD patterns of the selected gel samples.

laser power was typically 150 mW at the sample, and the resolution was 4 cm^{-1}.

All of the NMR, XRD, and Raman measurements were carried out at room temperature.

Results and Discussion

To obtain the information on the evaluation of long range ordering of the intermediate gel phases as a function of crystallization time, powder X-ray diffraction patterns were recorded, and the selected patterns are shown in Figure 1. For the initial gel without heating, the gel aged at 90 °C for 24 h, and the solid material produced by heating the aged gel at 200 °C for 50 min, their powder XRD patterns all looked identical and contain only an extremely broad signal, indicating that these solid phases are all X-ray amorphous. After heating the aged reaction mixture at 200 °C for 60 min, the corresponding XRD pattern shows three very weak reflection lines (Figure 1). The positions of these three peaks (especially the low-angle peak) do not coincide with the reflections of pure crystalline $AlPO_4$-11. In a previous study of gel chemistry of $AlPO_4$-11 synthesis, Tapp and co-workers observed metavariscite and variscite phases with poor crystallinity in the gel aged at 90 °C.[12a] However, these dense phases were not observed by Ren et al.[12b] Neither metavariscite nor variscite has reflections that mach the three lines observed in our study. It seems that a part of the amorphous material has evolved into an intermediate phase with certain

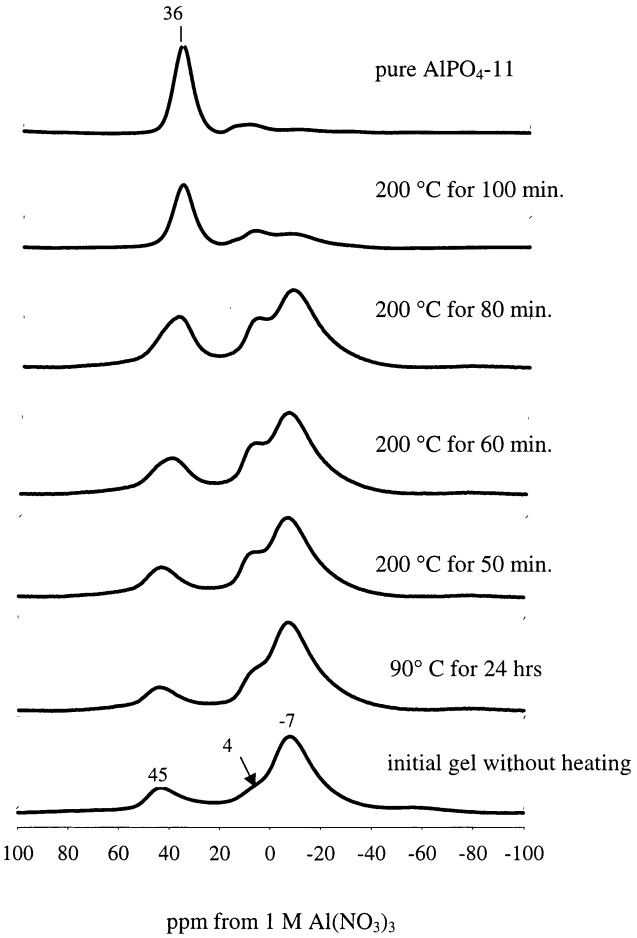

Figure 2. ^{27}Al MAS spectra of the selected gel samples.

degree of long range ordering. The fact that one of the reflections occurs in the region with very low 2θ value implies that this intermediate phase may have either a layered structure with large basal spacing or a microporous framework. Heating the gel at 200 °C for 80 min results in the appearance of reflections identical to that of pure crystalline $AlPO_4$-11. However, the intensities of the peaks due to $AlPO_4$-11 are very weak, which indicates that $AlPO_4$-11 crystallites just start forming. The XRD pattern also indicates that there is a very large amount of amorphous materials existing in the system. On the other hand, the three reflection lines seen in the XRD pattern of the 200 °C/60 min sample concomitantly disappeared, indicating that the species associated with the three reflections is not an impurity but a reactive intermediate which transforms into crystalline $AlPO_4$-11. Heating the aged gel at 200 °C for 100 min or longer yielded completely crystalline $AlPO_4$-11.

The ^{31}P and ^{27}Al MAS experiments were performed to probe the local chemical environments of P and Al atoms. The selected ^{27}Al and ^{31}P MAS spectra are shown in Figures 2 and 3. The ^{31}P and ^{27}Al MAS spectra of as-made $AlPO_4$-11 agree well with those reported in the literature.[13a] The ^{31}P and ^{27}Al MAS spectra of the gel heated at 200 °C for 100 min and longer looked very similar to those of pure crystalline $AlPO_4$-11. This suggests that heating the aged gel for more than 80 min results in almost pure $AlPO_4$-11 phase, which is consistent with the result of powder XRD. For the initial gel without heating, the ^{27}Al MAS spectrum contains a weak peak at around 45 ppm and a strong peak at −7 ppm with a prominent shoulder on the downfield side at about 4 ppm. On the basis of the shift value, the 45 ppm peak may be assigned to tetrahedral Al sites in the aluminophosphate (AlPO) species.[18] However, the simple MAS

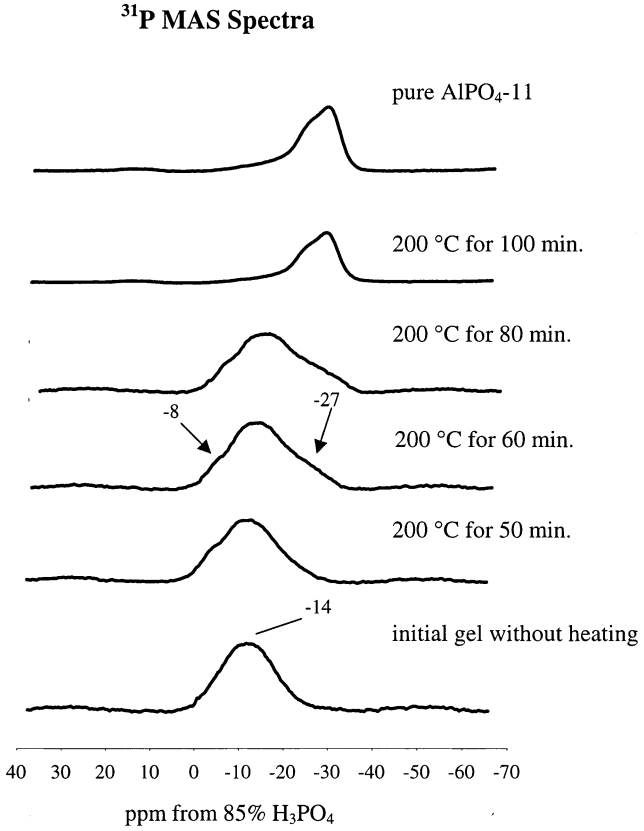

Figure 3. ^{31}P MAS spectra of the selected gel samples.

spectra alone do not provide direct evidence that this Al signal is connected to any phosphorous in the gel. The intensity of this peak increases with increasing the heating time. The position of this tetrahedral peak also gradually shifted with increasing heating time. The tetrahedral aluminum peak in crystalline $AlPO_4$-11 is 36 ppm, suggesting that there is a slight change in the chemical environment around the tetrahedral Al. The assignments for the main peak at −7 ppm and especially its downfield shoulder at 4 ppm are ambiguous. The −7 ppm peak may be assumed to be the framework octahedral Al sites in an AlPO material bound to water and PO_4 groups.[18] The shoulder at 4 ppm could be due to either the octahedral Al in unreacted alumina or five-coordinated Al in an AlPO gel. Further, it is unclear if these two maximums at −7 and 4 ppm are actually due to two separate peaks or just a single ^{27}Al resonance with asymmetric line shape resulting from a large quadrupolar coupling constant. The above-mentioned uncertainties will be dealt with shortly.

For the initial gel without heating, the ^{31}P MAS spectrum consists of a very broad resonance centered at around −14 ppm (Figure 3). The assignment of this −14 ppm peak is worth mentioning. In previous studies of several $AlPO_4$-based molecular sieve synthesis, the broad ^{31}P peaks in the range −10 to −20 ppm were usually observed in the gel samples obtained in the early stages of the crystallization.[19] These peaks were usually assigned to the amorphous AlPO species based on the ^{31}P chemical shifts of soluble aluminophosphate species in solution.[20] Again, there is no direct proof that these ^{31}P peaks are actually connected to the Al sites. In addition to aluminophosphates, several other phosphate species such as mono-, di-, and polyphosphates, hydrogen monophosphates, and dihydrogen phosphates can also appear in this region.[21] Heating the aged gel at 200 °C for 60 min resulted in the appearance of a new weak shoulder at about −27 ppm on the upfield side of the −14 ppm main peak. This new resonance does not belong to $AlPO_4$-11 because the ^{31}P MAS spectrum of as-made $AlPO_4$-11 exhibits only a single asymmetric peak at −31 ppm.[13a] Thus, the ^{31}P MAS spectra are consistent with the XRD results that a new intermediate phase exists in the gel heated at 200 °C for 60 min and that the $AlPO_4$-11 crystallites have not yet formed. This shoulder becomes more prominent and broader in the spectrum of the sample heated at 200 °C for 80 min. In the ^{31}P MAS spectra of 90 °C/24 h, 200 °C/50 min, 200 °C/60 min, and 200 °C/80 min samples, there is also a very weak shoulder at about −8 ppm on the downfield side of the −14 ppm main peak. The nature of this resonance is not immediately apparent from ^{31}P MAS spectra.

It is evident that the ^{31}P and ^{27}Al MAS spectra only provide limited structural information, and ambiguities do exist in spectral assignments. To better characterize the structure of the intermediate gel phases, we have further performed several other high-resolution solid-state NMR experiments. We first carried out the ^{27}Al 3QMAS experiments to clarify one of the ambiguities in the ^{27}Al MAS spectral assignment. In Figure 2, the ^{27}Al MAS spectra of the initial gel without heating, the gel samples of 90 °C/24 h, 200 °C/50 min, 200 °C/60 min, and 200 °C/80 min all contain a broad peak at −7 ppm with a shoulder at 4 ppm. As discussed earlier, it is not clear whether these two maximums are due to two different Al sites or just one resonance with asymmetric line shape. The limited resolution of simple ^{27}Al MAS is due to the fact that spinning at magic angle cannot completely eliminate the second-order quadrupolar interaction. Recently, a two-dimensional MQMAS experiment was developed for half-integer quadrupolar nuclei.[9] Because this method averages out second-order quadrupolar broadening completely, it provides much higher spectral resolution compared to congenital MAS experiment. Figure 4 illustrates the 3QMAS spectra of the initial gel without heating and 200 °C/60 min sample. Both spectra clearly show that there are three separate ^{27}Al resonance signals, indicating that the shoulder seen at 4 ppm in the simple ^{27}Al MAS spectrum is indeed due to an aluminum environment different from that represented by the strong peak at −7 ppm. The 3QMAS spectra of the gel samples heated at 90 °C/24 h and 200 °C/50 min were also obtained (not shown) and similar to that of the 200 °C/60 min sample described above. It is also noticed that the three peaks in isotropic (F1) dimension remain fairly broad, indicating the existence of a distribution of chemical shift and/or quadrupole-induced shift. This observation is consistent with the amorphous nature of the sample. Although higher resolution was achieved with 3QMAS, the question regarding the connectivity still remains; that is, whether the 4 ppm peak is due to the octahedral Al in unreacted alumina or a 5-coordinated Al site in AlPO species.

To address this problem and others presented below, we then carried out $^{27}Al \rightarrow {}^{31}P$ cross polarization experiments to select $^{27}Al-O-{}^{31}P$ connectivity in the gel samples. The cross polarization is mediated by direct through space heteronuclear dipolar interaction.[6a] Because this interaction strongly depends on the internuclear distance, the CP technique can be used to identify spatially adjacent molecular/atomic species. In zeolite synthesis, $^{1}H \rightarrow {}^{29}Si$[22] and $^{1}H \rightarrow {}^{2}H$[23] CP techniques have been used elegantly to yield important information on the intermolecular interactions between the template molecules and silicate species in the synthesis mixtures. In the present study, we have utilized two-dimensional (2D) heteronuclear chemical shift correlation spectroscopy (HETCOR), a 2D technique based on cross-polarization,[24] to obtain a correlation map of resonances from proximal nuclei. We first examined the initial gel without

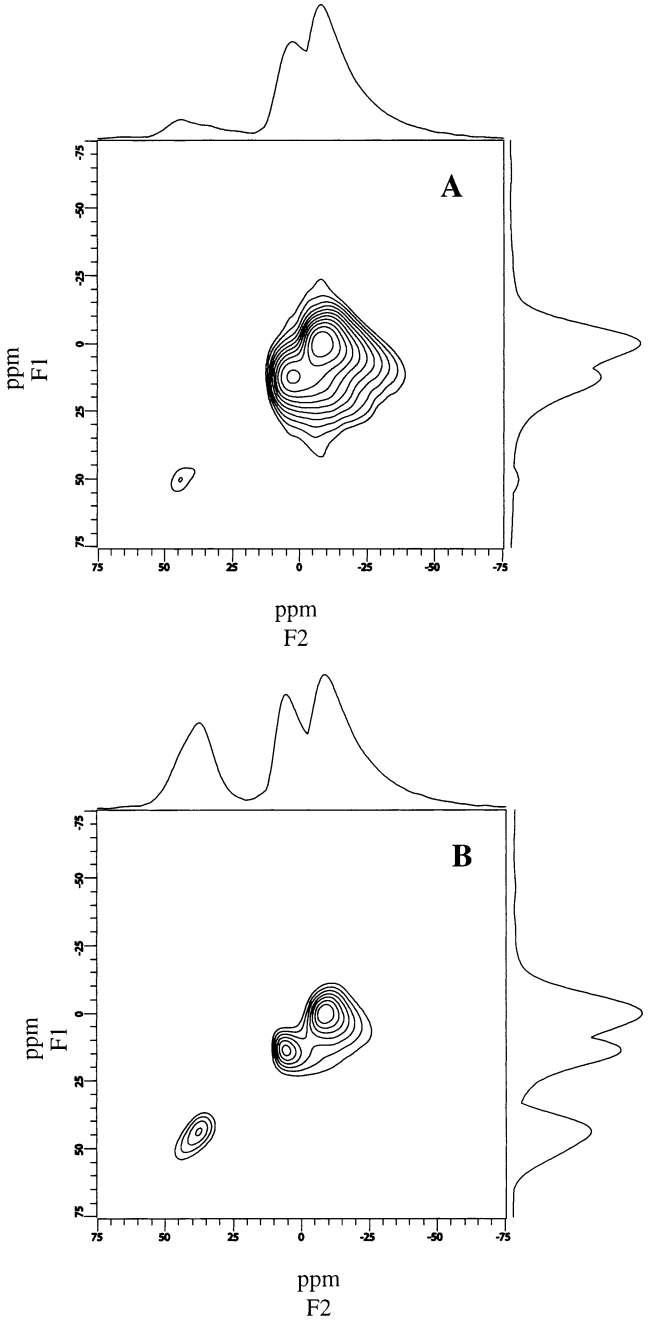

Figure 4. ^{27}Al 3QMAS spectra (9.4 T) of **(**A**)** the initial gel without heating and **(**B**)** the gel heated at 200 °C for 60 min. Both spectra were obtained using a spinning rate of 20 kHz; a t_1 increment of 25 μs and a total of 32 t_1 increments. 2040 scans were acquired for both **(**A**)** and **(**B**)** with a repetition delay of 0.5 s.

heating. The ^{31}P MAS spectrum (Figure 3) of the initial gel without heating exhibits a broad resonance at −14 ppm. As mentioned earlier, the chemical environment of this peak is ambiguous, which arises from the fact that the phosphorus atoms in a number of phosphates and aluminophosphates can both exhibit similar chemical shifts. A previous study of $AlPO_4$-11 synthesis suggested that mixing the aluminum oxide with phosphoric acid and organic amine at room temperature only results in precipitation of aluminum oxide hydrate in a more reactive colloidal form that serves as a precursor for further reaction and that the subsequent pretreatment of the gel precursor at 90 °C converts this form of aluminum oxide hydrate to aluminophosphate complexes which eventually lead to microporous $AlPO_4$-11.[12b] The implication is that there would be no significant reaction between Al and P sources at room temperature. If this were the case, there should be no AlPO species existing in the initial gel and, therefore, the ^{31}P peak at −14 ppm would not be connected to any of the Al sites observed in the ^{27}Al MAS spectrum. Figure 5 illustrates the ^{27}Al → ^{31}P HETCOR spectrum of initial gel without heating, from which the above-mentioned ambiguity is immediately clarified. The ^{31}P projection contains a broad CP signal at −14 ppm corresponding to the peak seen in the MAS spectrum. The connectivity shown in the HETCOR spectrum provides direct proof that this broad ^{31}P signal is connected to aluminum via a dipolar interaction. In the ^{27}Al projection, two peaks are observed at +45 and −7 ppm. The shoulder at 4 ppm appearing in the corresponding ^{27}Al MAS spectrum does not show up in the projection, indicating that this resonance is due to the unreacted aluminum oxide and not five-coordinated Al in the AlPO gel. The broad peak at −14 ppm in the ^{31}P projection is correlated to both tetrahedral and octahedral ^{27}Al peaks at +45 and −7 ppm, respectively. Our results clearly show that mixing Al and P sources together with the structure-directing agent at room temperature does yield a significant amount of amorphous AlPO species. Both tetrahedral and octahedral Al sites are present in this AlPO material, and both are connected to the P atoms at −14 ppm. Careful inspection of 2D spectrum reveals that the broad peak at −14 ppm in the ^{31}P projection actually encompasses two components. The first component is a weak ^{31}P resonance at −18 ppm, which is only connected to the ^{27}Al peak at 45 ppm. It represents a small amount of phosphorus atoms with only tetrahedral aluminum as the nearest neighbors. The second component is the broad peak at −14 ppm connected to both tetrahedral and octahedral Al sites. These connectivities can be seen more clearly in the ^{31}P slices taken through the tetrahedral and octahedral Al sites (Figure 5). These two components are apparently due to the P atoms with different degrees of condensation. The fact that the −14 ppm main peak is connected to both tetrahedral and octahedral aluminum sites indicates that this tetrahedral phosphorus must have, at least, two aluminum atoms in its second coordination sphere. In the literature, most of the reported chemical shifts of ^{31}P in $AlPO_4$-based microporous materials fall in the range −19 to −31 ppm and are assigned to tetrahedral phosphorus bound to four aluminum atoms via bridging oxygen, $P(OAl)_4$.[18] The broad peak at −14 ppm is outside this range, implying that the number of aluminum atom in the second coordination shell is either two or three, but less than four. Sayari et al. have pointed out that the presence of P−OH groups can cause a downfield shift of a ^{31}P signal in AlPO-based materials.[18a] Thus, we assign the −14 ppm peak to phosphorus atoms with mixed coordination $P(OH)_x[OAl(tet)]_y[OAl(oct)]_{4-(x+y)}$ where $x = 1$ or 2. The presence of P−OH groups is also supported by ^{1}H → ^{31}P cross polarization results, which will be presented momentarily. The peak at −18 ppm connected to only tetrahedral Al sites is also worth a few words of discussion. Sayari et al. further suggested that the chemical shift of ^{31}P in AlPO species changes additively with the number of surrounding aluminum atoms in the second coordination sphere of phosphorus.[18a] In addition, for AlPO materials, the ^{31}P chemical shifts of the phosphorus sites with highly coordinated aluminum such as octahedral Al in their second coordination sphere are further downfield compared to the P sites bound only to 4-corrdinated Al. Using this argument and knowing that the P site at −14 ppm is connect to at least one tetrahedral and one octahedral Al, we can conclude that the phosphorus at −18 ppm must have at least two tetrahedral Al atoms in its second coordination sphere.

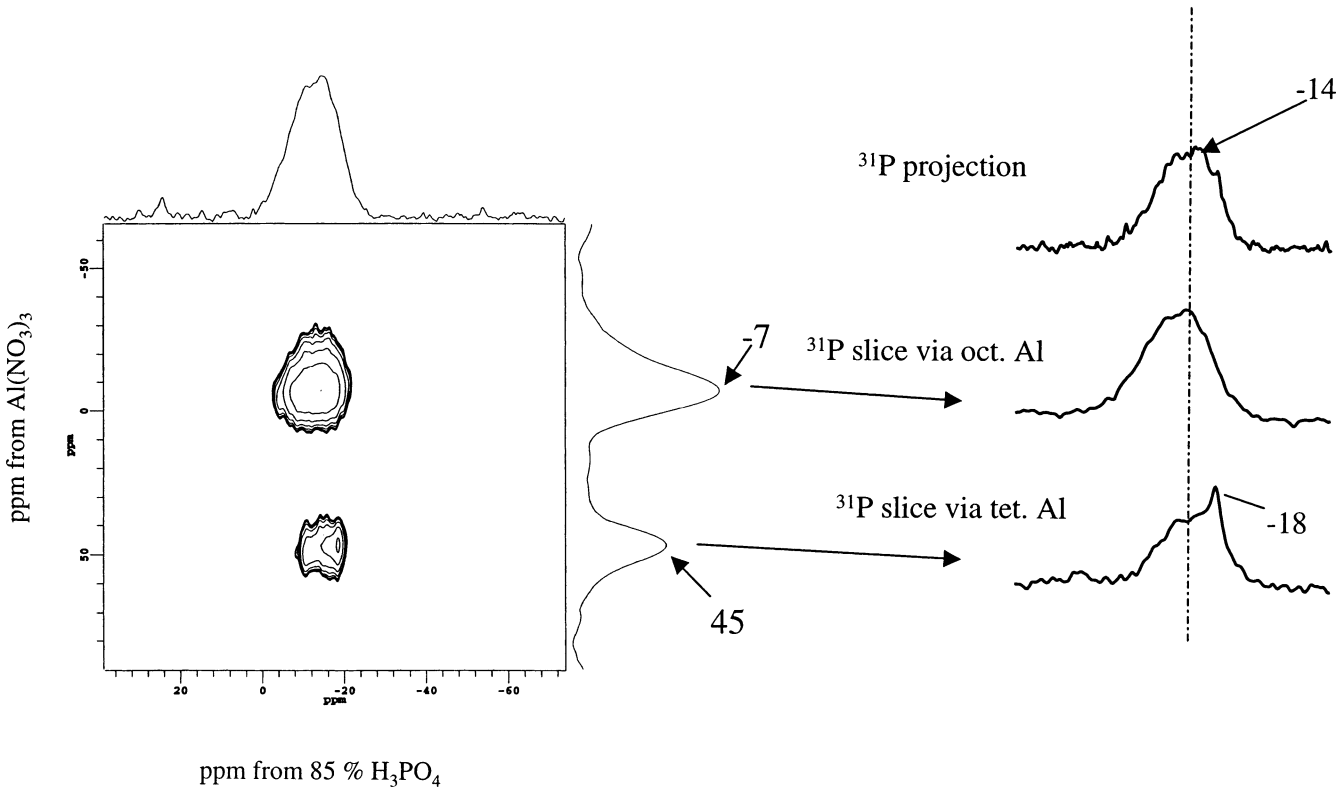

Figure 5. $^{27}Al \rightarrow {}^{31}P$ HETCOR spectrum of the initial gel with a contact time of 0.8 ms. For each of the 48 experiments in t_1, 6000 scans were acquired. The spinning rate was 7 kHz.

We have carefully examined another representative gel sample obtained by heating the aged mixture at 200 °C for 60 min. This is the gel sample whose powder XRD pattern shows the appearance of a semicrystalline reactive intermediate phase that is quickly converted to $AlPO_4$-11. The $^{27}Al \rightarrow {}^{31}P$ HETCOR spectrum of 200 °C/60 min sample is shown in Figure 6. Both tetrahedral and octahedral aluminum sites were observed in the ^{27}Al projection and, therefore, are connected to P sites. The 4 ppm shoulder seen in the ^{27}Al MAS spectrum did not appear, implying again that this shoulder is an independent Al site, which is also consistent with the ^{27}Al 3QMAS spectrum presented earlier. This site is not part of the AlPO species, suggesting a significant amount of unreacted Al source still exists. A broad ^{31}P peak at -15 ppm observed in the ^{31}P projection is connected to both tetrahedral and octahedral Al sites. The chemical shift of this ^{31}P peak is almost identical to that of the initial gel without heating. Thus, as discussed earlier, this broad resonance represents P atoms that are not fully condensed. Careful examination of the spectrum reveals that there are actually two different types of tetrahedral aluminum sites centered at 45 and 38 ppm, respectively. The ^{31}P resonance at -15 ppm only correlates to the tetrahedral aluminum at 45 ppm which coincides with the shift of the tetrahedral aluminum in the initial gel without heating. These results suggest that the ^{31}P resonance at -15 ppm originates from phosphorus that is not fully condensed and belongs to an amorphous AlPO species very similar to that observed in the initial gel without heating. The downfield weak shoulder at around -8 ppm seen in the ^{31}P MAS spectrum did not show up in the 2D spectrum, indicating that it is probably due to phosphorus in an unknown amorphous material that has no aluminum in close vicinity. The upfield shoulder observed at -27 ppm in the corresponding ^{31}P MAS spectrum now appears as a well-resolved peak in the ^{31}P projection. We attribute this peak to phosphorus in the semicrystalline reactive intermediate phase. As stated earlier, the reported ^{31}P chemical shifts of phosphorus in vast majority of microporous $AlPO_4$-based materials fall in the range from -19 to -31 ppm and are due to tetrahedral phosphorus covalently bonded to four aluminum via bridging oxygen. This suggests that the ^{31}P resonance at -27 ppm in the reactive intermediate phase is due to fully condensed phosphorus atoms with the environment of $P(-OAl)_4$. The 2D spectrum shows that the four Al atoms in the second coordination sphere are all tetrahedral Al sites and the shift of this tetrahedral Al site is at 38 ppm which is close to that of as-made $AlPO_4$-11.

The $^{27}Al/^{31}P$ double resonance experiments also provide direct evidence that the ^{31}P peak at -27 ppm represents the phosphorus atoms with higher degree of condensation compared to the ^{31}P peak at -15 ppm. A comparison of ^{31}P MAS and ^{31}P projection of HETCOR spectrum reveals that the intensity of the peak at -27 ppm was more enhanced by cross polarization relative to the -15 ppm main peak. Fyfe and co-workers have carried out the $^{27}Al \rightarrow {}^{29}Si$ CP on various zeolites and found that the relative enhancement of ^{29}Si signals is linear with the number of Al atoms in neighboring T sites (T = Si and Al).[25] If this argument is accepted, in the present case, the larger enhancement of the ^{31}P peak at -27 ppm is consistent with our assignment based on chemical shift that this ^{31}P peak is due to fully condensed $P(-OAl)_4$ environment and results from a larger $^{31}P-{}^{27}Al$ dipole−dipole interaction, whereas -15 ppm is due to partially condensed P sites (where the number of Al atoms in the second coordination sphere is less than 4). However, care must be exercised when interpreting CP intensity because cross polarization involving a quadrupolar nucleus such as ^{27}Al ($I = 5/2$) can be inefficient because of the difficulty in spin-locking. For quadrupolar nuclei with half-integer spins, Vega has first demonstrated that spin-locking of the central transition is affected by the time dependence of the first-order quadrupolar

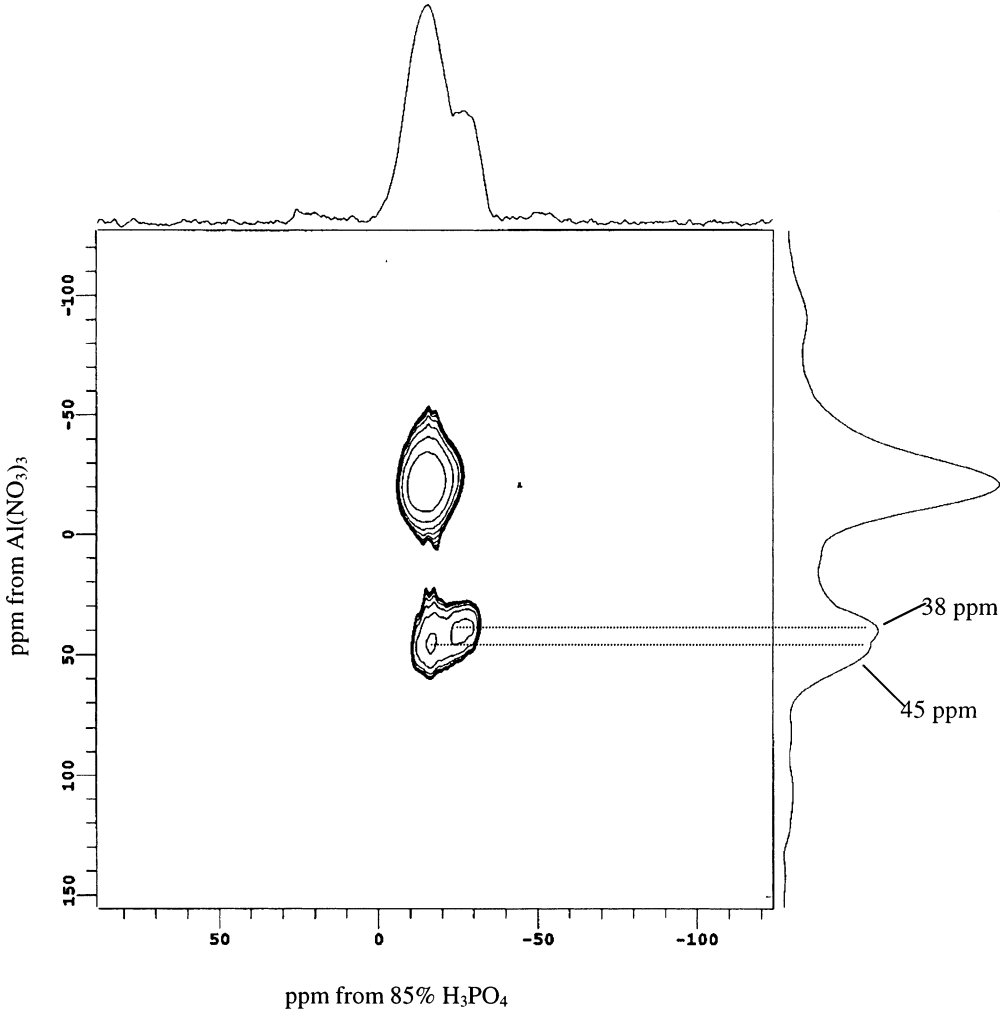

Figure 6. $^{27}Al \rightarrow {}^{31}P$ HETCOR spectrum of the gel sample heated at 200 °C for 60 min with a contact time of 1 ms. For each of the 40 experiments in t_1, 16 000 scans were acquired. The spinning rate was 6 kHz.

splitting under MAS conditions.[16,26] The spin-locking efficiency is low in the intermediate regime between sudden and adiabatic passage of the zero-energy crossings of the first-order quadrupolar splitting. A study by De Paul et al. has further shown that even well in the sudden-passage regime it is not always possible to spin-lock the central transition of quadrupolar nuclei in a powder.[27] For this reason, we further preformed ^{31}P $\{^{27}Al\}$ TRAPDOR and REDOR experiments to check the CP results. These particular double resonance experiments are designed to measure dipolar interactions between two unlike spins under MAS conditions. Therefore, they also provide connectivity information but do not involve coherence transfer and spin-locking. We measured the TRAPDOR and REDOR spectra of the 200 °C/60 min sample as a function of dephasing time. Figure 7 illustrates the selected ^{31}P spin−echo (S_0), TRAPDOR (S), and TRAPDOR difference (ΔS) spectra. The normal spin−echo spectra of the control experiments show that the intensity of the ^{31}P peak at −15 ppm decreases much faster with increasing the echo time compared to the peak at −27 ppm, indicating that the amorphous material has a much shorter ^{31}P T_2 than that of the semicrystalline component in the sample. In the normal ^{31}P spin−echo spectrum with a total echo time of 3.33 ms, the −27 ppm peak which appears in the MAS spectrum as a very weak shoulder now has much larger intensity relative to the −15 ppm main peak because a longer echo time discriminates in favor of the ^{31}P signal with long T_2. The corresponding TRAPDOR difference spectrum (ΔS) further confirms that this phosphorus site is indeed coupled to aluminum. To qualitatively compare the strengths of dipolar interactions between the two different phosphorus sites and aluminum, we have to look at the spectra obtained with short dephasing times because the two ^{31}P resonances have very different T_2 values. The TRAPDOR difference spectrum obtained with a short Al irradiation time of 0.167 ms illustrates clearly that the intensity of the −27 ppm peak is significantly enhanced relative to the −15 ppm peak. For microporous $AlPO_4$-based molecular sieves and aluminophosphates glasses, the Al−O−P distance is normally around 3 Å (yielding $^{27}Al-{}^{31}P$ dipolar coupling constants in the range of 400−500 Hz). As pointed out by van Eck et al., the Al−O−P distances in these aluminophosphates only vary slightly;[28] thus, we believe that the larger TRAPDOR effect observed for −27 ppm peak is likely due to that the number of aluminum atoms in the second coordination sphere is higher than that for the phosphorus appearing at −15 ppm. The REDOR experiments yielded essentially the same information (the spectra are not shown). Therefore, the results of TRAPDOR and REDOR experiments are consistent with the results from $^{27}Al \rightarrow {}^{31}P$ CP experiments. These $^{27}Al/^{31}P$ double resonance experiments provide direct evidence that the −27 ppm peak represents the highly condensed phosphorus atoms.

We have also conducted the $^{1}H \rightarrow {}^{31}P$ CP on this gel sample. Figure 8A shows the selected CP spectra. The spectrum with a short contact time of 0.1 ms contains a peak at −15 ppm. It looks similar to the corresponding ^{31}P MAS spectrum except

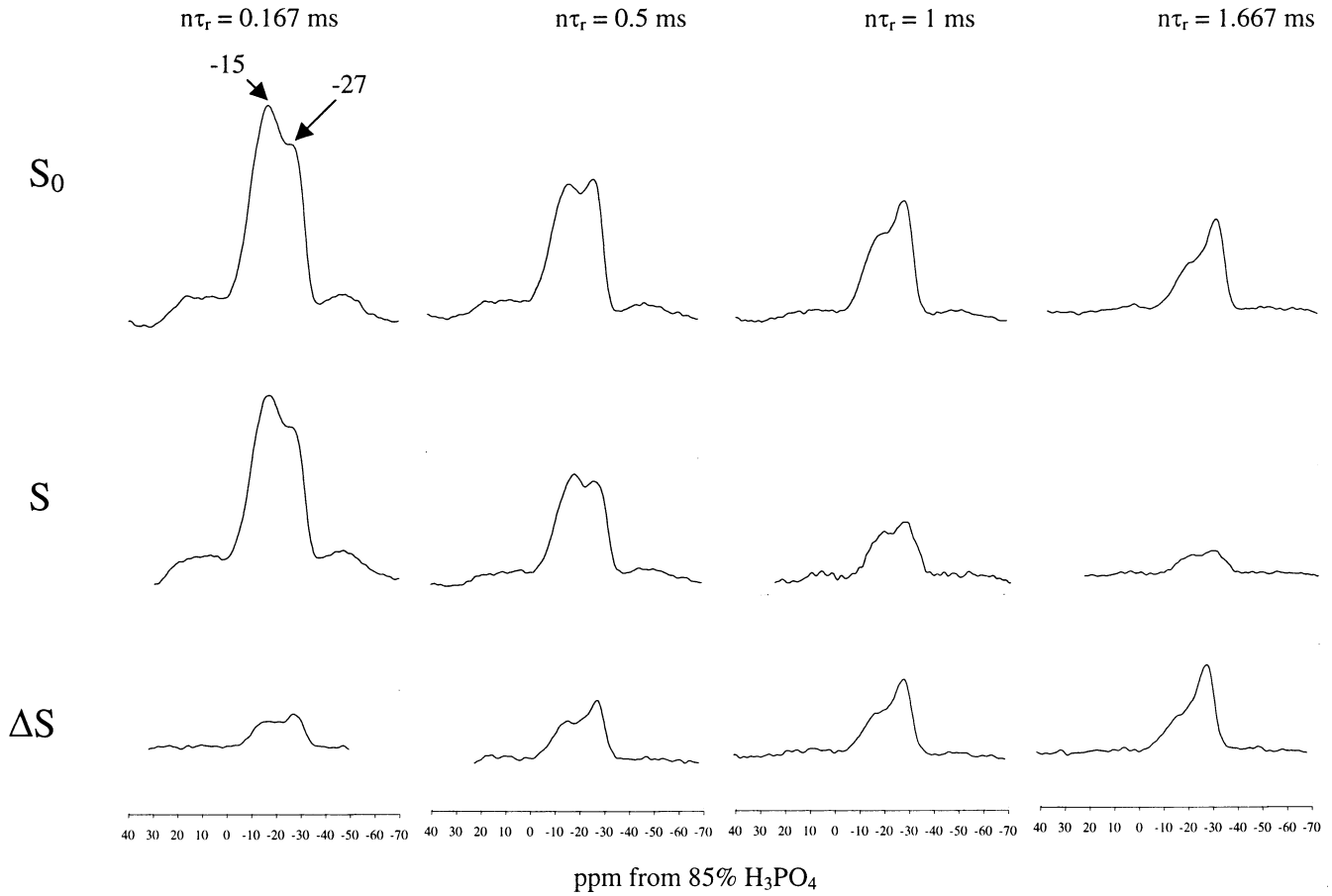

Figure 7. Selected ^{31}P {^{27}Al} TRAPDOR spectra of the gel sample heated at 200 °C for 60 min. Top row: spectra with no ^{27}Al irradiation, S_0 (the control experiment). Middle row: spectra with ^{27}Al irradiation, S. Bottom row: difference spectra, ΔS.

that the weak shoulder at −27 ppm is less obvious. The CP spectrum with a long contact time (10 ms) apparently discriminates in favor of the peak at −27 ppm. However, it is not clear if the discrimination is mainly through the difference in the proton−phosphorus dipolar interactions or the difference in $T_{1\rho}^{H}$ (proton spin−lattice relaxation time in the rotating frame of reference) values of two coexisting phases. The severe overlap of two resonance signals precludes us from analyzing the cross polarization dynamics for each individual site separately. Instead, as an aid to interpreting the CP data, we carried out variable CP contact time measurements of as-made $AlPO_4$-11, and the initial gel without heating which contains predominately amorphous materials. Variation of CP signal intensities for these two samples as a function of contact time is shown in Figure 8, parts B and C. The initial growth of the CP signal is governed by the cross polarization time constant (T_{CP}) that is proportional to the second moment of the dipolar coupling between the source and target spins. The decay of the magnetization at longer contact times is dictated by the $T_{1\rho}^{H}$. Figure 8, parts B and C, shows that the signal decay is much faster for the initial gel due apparently to its much shorter $T_{1\rho}^{H}$. The CP dynamics can be described by

$$S(t) = S_{max}(1 - T_{CP}/T_{1\rho}^{H})^{-1}[\exp(-\tau/T_{1\rho}^{H}) - \exp(-\tau/T_{CP})]$$

Fitting the curves to the equation yields $T_{1\rho}^{H}$ values of 25 and 2.7 ms, and T_{CP} values of 0.65 and 0.47 ms for the ^{31}P signal of the as-made $AlPO_4$-11 and amorphous AlPO material in initial gel, respectively. Assuming that the CP behavior of the phosphorus sites at −27 ppm (semicrystalline domain) and −15 ppm (amorphous domain) in the sample of 200 °C/60 min resembles that of the crystalline as-made $AlPO_4$-11 and amorphous AlPO material in the initial gel, respectively, it seems that for the 200 °C/60 min sample, the selectivity in CP spectra using long contact times is mainly due to that the semicrystalline component in this heterogeneous sample has a much longer $T_{1\rho}^{H}$ value. The relatively short T_{CP} value for phosphorus sites in the amorphous AlPO gel confirms our privous suggestion that the P site has directly attached OH groups, $P(OH)_x[OAl(tet)]_y[OAl(oct)]_{4-(x+y)}$ where $x = 1$ or 2. For as-made $AlPO_4$-11, the proton reservoir for cross polarization is the template amine molecules, and the water molecules occluded inside the channels are likely too mobile at room temperature to act as the source for magnetization transfer. A relatively short T_{CP} value for as-made $AlPO_4$-11 indicates that there is a significant dipolar interaction between the protons of dipropylamine and framework P atoms, which is consistent with that the channel dimension of $AlPO_4$-11 is rather small, resulting in the reduced the mobility of the template molecules inside the pores and, therefore, more efficient polarization transfer. The interpretation is also consistent with our and other's[29] observation that dipropylamine can be neither washed out from the channels nor extracted under vacuum.

We also further characterized the gel sample heated at 200 °C for 50 min. The formation of a reactive semicrystalline intermediate is clearly evident from the XRD pattern of the aged mixture treated at 200 °C for 60 min. Although the gel sample heated at 200 °C for 50 min is completely X-ray amorphous (Figure 1), it is possible that the sample contains crystallites of the above-mentioned intermediate whose size may be too small to be detected by the X-ray diffraction. Unlike the 200 °C/60 min sample, the ^{31}P MAS spectrum of 200 °C/50 min sample

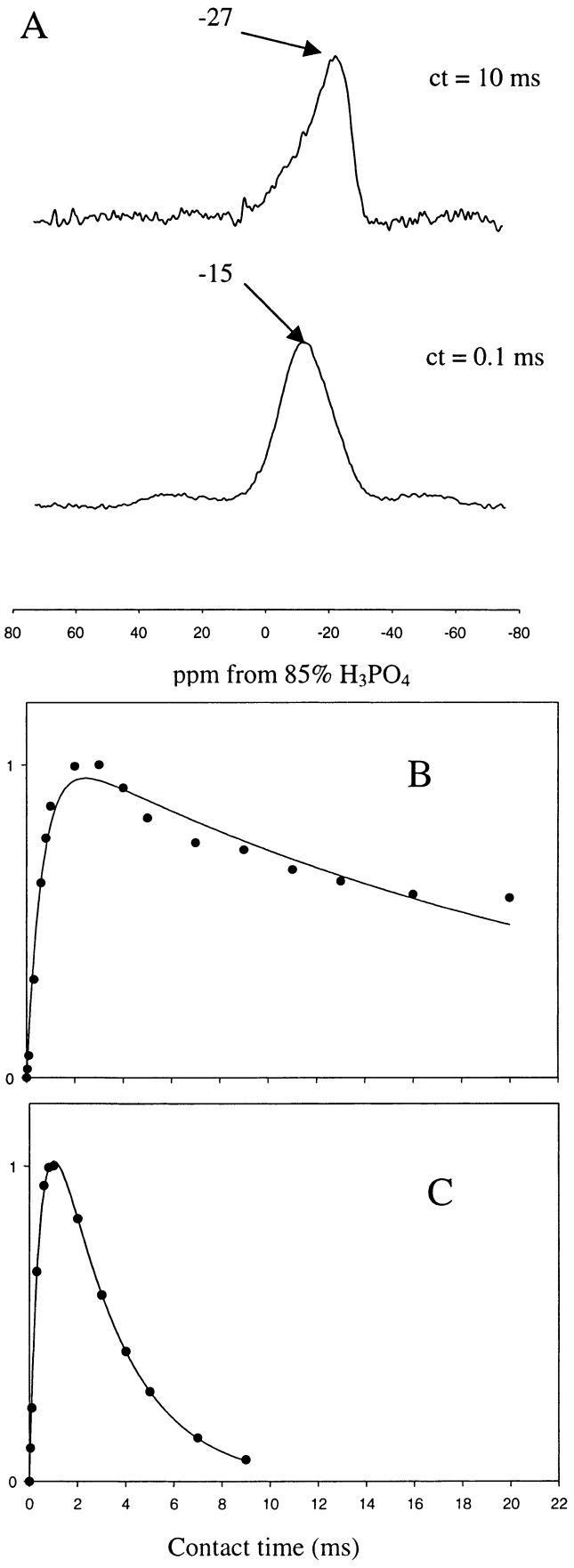

Figure 8. (A) $^1H \rightarrow {}^{31}P$ CP spectra of the gel sample heated at 200 °C for 60 min with different contact times. Variation of the intensities of the $^1H \rightarrow {}^{31}P$ CP signals as a function of the contact time for (B) as-made $AlPO_4$-11 and (C) the initial gel without heating.

did not exhibit an obvious shoulder at abound −27 ppm. However, the breadth of the broad amorphous peak does cover the region where the peak due to the reactive intermediate appears. Thus, a small ^{31}P resonance signal due to the reactive semicrystalline intermediate might be buried underneath the very large amorphous peak. If this is the case, the spectral editing techniques such as $^1H \rightarrow {}^{31}P$ CP and $^{31}P/^{27}Al$ double resonance experiments may help to identify the existence of the possible semicrystalline intermediate phase. Figure 9A shows the selected $^1H \rightarrow {}^{31}P$ CP spectra. The CP spectrum with a short contact time exhibits a single peak centered at −14 ppm similar to that in ^{31}P MAS spectrum, but its width is apparently narrower. The CP spectrum with a longer contact time of 9 ms does display a new signal appearing as an obvious shoulder at around −23 ppm on the upfield side of the −14 ppm main peak. On the basis of the previous discussion, the two ^{31}P resonance signals are likely due to two phases in the sample with different $T_{1\rho}^{H}$ values. Figure 9B illustrates the selected ^{31}P $\{^{27}Al\}$ REDOR difference spectra. The spectrum with a long dephasing time also contains a peak at −14 ppm and a prominent shoulder at around −23 ppm. This shoulder with a longer ^{31}P T_2 was not observed in the corresponding ^{31}P MAS spectrum. Observation of this −23 peak in the REDOR difference spectrum further confirms that this resonance is connected to the aluminum. Thus, the $^1H \rightarrow {}^{31}P$ CP and ^{31}P $\{^{27}Al\}$ REDOR experiments indicate that the 200°C/50min sample comprises two AlPO phases: (1) an amorphous phase characterized by a ^{31}P peak at −14 ppm and (2) a second domain whose NMR properties such as long ^{31}P T_2 and ^1H $T_{1\rho}$ are similar to those of the semicrystalline intermediate observed in the 200 °C/60 min sample. This domain was not directly detected by XRD and simple ^{31}P MAS NMR.

The early work by Dutta and co-workers has established Raman spectroscopy as an important tool for the investigation of the crystallization of zeolitic materials.[30] In the present work, we have also used FT-Raman spectroscopy to further obtain the information on the intermediate gel phases. The selected FT-Raman spectra are shown in Figure 10. To assist identification of the vibrational bands due to the template molecules, the FT-Raman spectrum of pure di-*n*-propylamine (DPA) was also included in the figure. The vibrational bands due to the template are clearly seen in the spectra of the gel aged at 90 °C and the solids obtained by subsequently heating at 200 °C as well as as-made $AlPO_4$-11 even after repeatedly washing, implying that for these solids the template molecules are occluded in the AlPO species. However, the FT-Raman spectrum of the initial gel without heating does not contain any Raman bands due to DPA. These results indicate that, although an amorphous AlPO material is formed immediately after mixing Al and P sources in the presence of the template as indicated by solid-state NMR results, the template molecules neither are incorporated in the AlPO material tightly nor interact with the AlPO species strongly. The FT-Raman spectrum of as-made $AlPO_4$-11 is in good agreement with those reported previously.[31] One particular band in the spectrum is worth mentioning. A sharp peak positioned at 262 cm^{-1} was previously identified by Holmes et al. as the $AlPO_4$-11 framework vibration.[31] They assigned this band to the 10-membered ring breathing mode. Figure 10 shows that this peak was clearly observed in the spectrum of the 200 °C/100 min sample whose XRD pattern indicates the pure $AlPO_4$-11 is the predominate product. The peak is also present in the spectrum of the 200 °C/80 min sample, but its intensity is extremely weak. This is consistent with the corresponding XRD pattern showing that the solid contains a small amount of $AlPO_4$-11 and a large amount of amorphous materials. Interest-

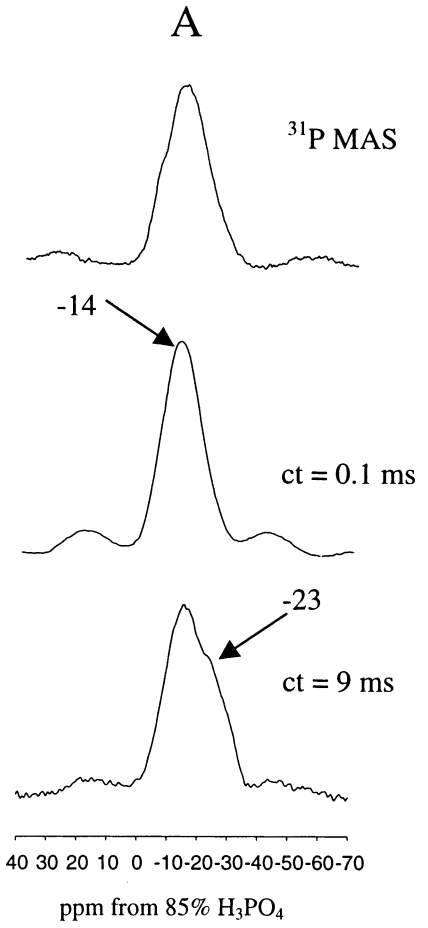

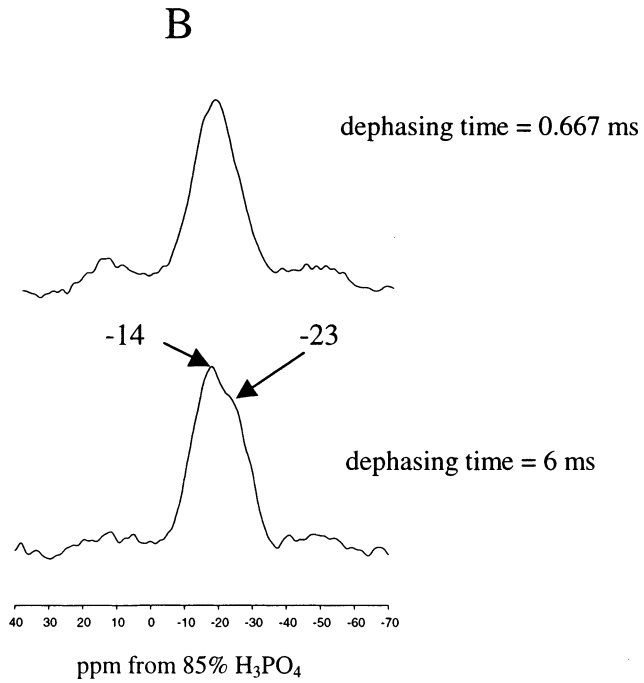

Figure 9. (A) ^{1}H → ^{31}P CP spectra of the gel sample heated at 200 °C for 50 min with different contact times. (B) Selected ^{31}P {^{27}Al} REDOR difference spectra of the gel sample heated at 200 °C for 50 min with different dephasing times.

ingly, this peak did not appear in the spectra of the 200 °C/60 min, 90 °C/24 h, and the initial gel without heating. It suggests that the 10-mmbered ring channel system does not exist in the AlPO-based reactive semicrystalline intermediate observed in the 200 °C/60 min sample and the amorphous AlPO material.

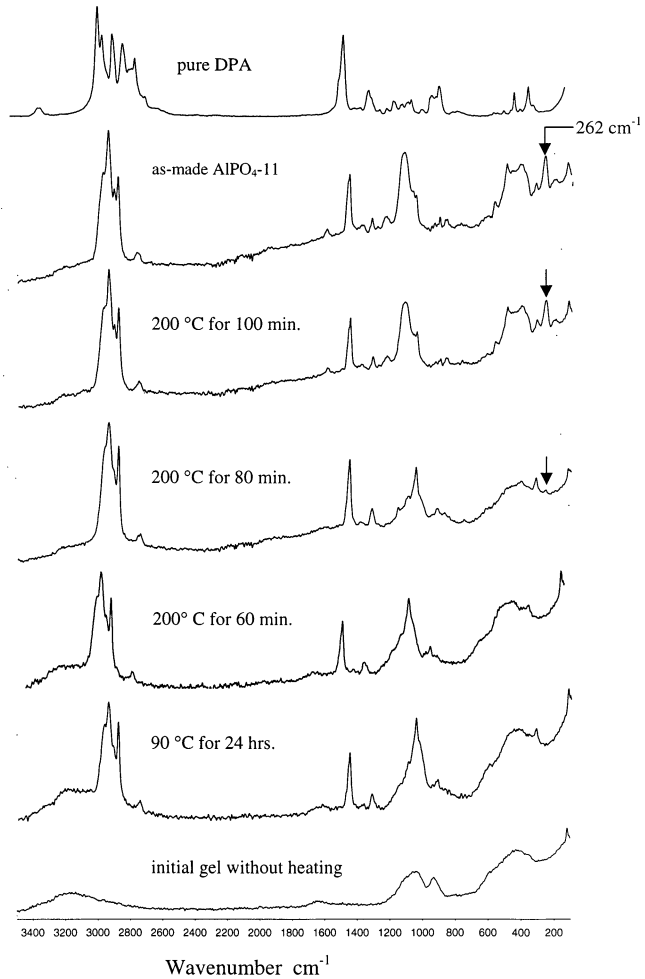

Figure 10. FT-Raman spectra of the selected gel samples

Summary

We have examined the evolution of the gel phases as a function of crystallization time by solid-state NMR in conjunction with powder XRD and FT-Raman spectroscopy. We have carefully characterized several representative solid gel phases obtained at several different stages of the reaction using a number of dipolar-coupling based solid-state NMR techniques. In contrast to previous reports, we found that under the experimental conditions employed, aluminophosphate species does exist in the initial gel formed at room temperature as detected unambiguously by ^{27}Al → ^{31}P CP experiments. The different P and Al sites were identified and their connectivity mapped out by ^{27}Al/^{31}P HETCOR experiments. The FT-Raman spectrum indicates that there is little interaction between template molecule and the AlPO gel at this stage. For the solid sample heated at 200 °C for 60 min, the ^{1}H → ^{31}P CP confirms the existence of a semicrystalline reactive intermediate phase suggested by powder XRD pattern. The results of the ^{27}Al → ^{31}P CP, ^{31}P {^{27}Al} TRAPDOR, and REDOR experiments show that the ^{31}P atoms in this intermediate phase are highly condensed. The ^{1}H → ^{31}P CP and ^{31}P {^{27}Al} REDOR data further suggests that this reactive intermediate (or the precursor of the reactive intermediate phase) also exists in the solids heated at 200 °C for 50 min despite that it is not detected by either powder XRD or the simple ^{31}P MAS NMR. The NMR results show that during the crystallization, there is clearly an evaluation of a second AlPO domain coexisting with the amorphous AlPO material, which is indicated by the change in its ^{31}P shift (Figure 11). It should be pointed out that, in the early stages of the

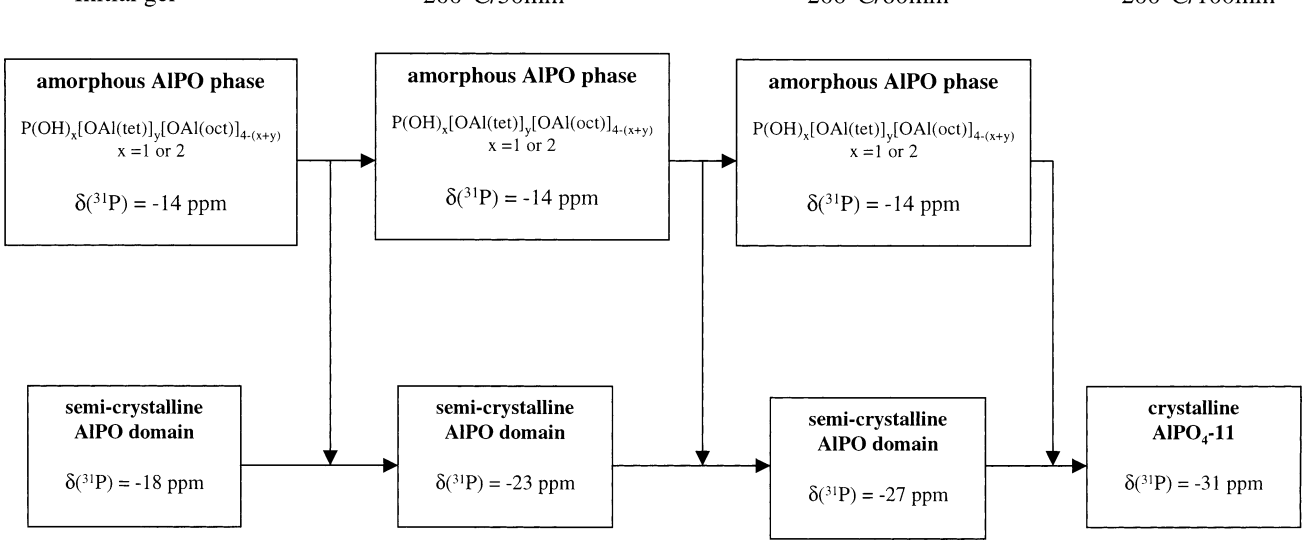

Figure 11. Evaluation of the semicrystalline AlPO domain as an intermediate coexisting with amorphous AlPO phase as a function of time

evolution, this ^{31}P site could only be followed by dipolar-coupling based double resonance NMR techniques. The FT-Raman spectra further indicate that the 10-membered ring channel system does not exist in the semicrystalline intermediate phase or the amorphous AlPO species. In this work, we have presented a number of cases where the dipolar-coupling based double resonance techniques can provide important connectivity information regarding the structures of the gels, which are not readily available from the simple MAS techniques.

We wish to point out that molecular sieve crystallization is an extremely complicated process, and the details about the formation of $AlPO_4$-11 are still not known. However, being able to better characterize the structure of intermediate gel phases using a umber of solid-state NMR techniques as demonstrated in the present study is a step forward toward the better understanding of the self-assembly processes of microporous materials at a molecular level.

Acknowledgment. Y.H. acknowledges the financial support from Natural Science and Engineering Research Council of Canada for a research grant and the funding for the purchase of a FT-Raman spectrometer. He also thanks the Canada Foundation for Innovation (CFI) for the award of a 400 MHz solid-state NMR spectrometer. R.R. thanks OGSST for a scholarship. All NMR spectra were acquired at the University of Western Ontario NMR Facility.

References and Notes

(1) Wilson, S. T.; Lock, B. M.; Messina, C. A.; Cannan, T. R.; Flanigen, E. M. *J. Am. Chem. Soc.* **1982**, *104*, 1146.

(2) (a) Gies, H.; Marler, B.; Werthmann, U. in *Molecular Sieves: Science and Technology*; Karge, H. G., Weitkamp, J., Eds.; Springer: Berlin, 1998; pp 35−64, Vol. 1. (b) Davis, M. E.; Lobo, R. F. *Chem. Mater.* **1992**, *4*, 756. (c) Francis, R. J.; O'Hare, D. *J. Chem. Soc., Dalton Trans.* **1998**, 3133. (d) Oliver, S.; Kuperman, A.; Ozin, G. A. *Angew. Chem., Int. Ed. Engl.* **1998**, *37*, 46. (e) Szostak, R. *Molecular Sieves: Principles of Synthesis and Identification*, 2nd ed.; Blackie Academic & Professional: London, 1998. (f). Wilson, S. T. In *Introduction to Zeolite Science and Practice*, 2nd ed.; van Bekkum, H., Flanigen, E. M., Jacobs, P. A., Jansen, J. C., Eds.; Elsevier: Amsterdam, 2001; p 229. (g) Lobo, R. F.; Zones, S. I.; Davis, M. E. *J. Inclusion Phenom. Mol. Recognit. Chem.* **1995**, *21*, 47. (h) Davis, M. E.; Zones, S. I. *Chem. Ind.* **1997**, *69*, 1. (i) Feng, S.; Xu, R. *Acc. Chem. Res.* **2001**, *34*, 239.

(3) (a) Engelhardt, G.; Michel, D. *High-Resolution Solid-State NMR of Silicates and Zeolites*; Wiley: Chichester, U.K., 1987. (b) Engelhardt, G. in ref 2f, pp 387. (c) Bell, A. T. In *Zeolite Synthesis*; ACS Symposium Ser. 398; Occelli, M. L., Robson, H. E., Eds.; American Chemical Society: Washington, DC, 1989; p 66.

(4) Barrie, P. J. In *Spectroscopy of New Materials*; Clark, R. J. H., Hester, R. E., Eds.; John Wiley & Sons: Chichester, U.K., 1993; pp 151.

(5) Huang, Y.; Machado, D. *Micropor. Mesopor. Mater.* **2001**, *47*, 195.

(6) (a) Pines, A.; Gibby, M. G.; Waugh, J. S. *J. Chem. Phys.* **1973**, *59*, 569. (b) Fyfe, C. A.; Mueller, K. T.; Grondey, H.; Wong-Moon, K. C. *J. Phys. Chem.* **1993**, *97*, 13484.

(7) (a) Grey, C. P.; Veeman, W. S.; Vega, A. J. *J. Chem. Phys.* **1993**, *98*, 7711. (b) Grey, C. P.; Vega, A. J. *J. Am. Chem. Soc.* **1995**, *117*, 8232. (c) van Eck, E. R. H.; Janssen, R.; Mass, W. E. J. R.; Veeman W. S. *Chem. Phys. Lett.* **1990**, *174*, 428.

(8) (a) Gullion, T.; Schaefer, J. *J. Magn, Reson.* **1989**, *81* 196. (b) Gullion, T.; Schaefer, J. *Adv. Magn. Reson.* **1989**, *13*, 57.

(9) Frydman, L.; Harwood, J. S. *J. Am. Chem. Soc.* **1995**, *117*, 5367.

(10) Wilson, S. T.; Lok, B. M.; Flanigen, E. M. U.S. Pat. 4,310,440, 1982.

(11) a) Bennett, J. M.; Richardson, J. W., Jr.; Pluth, J. J.; Smith, J. V. *Zeolites* **1987**, *7*, 160. (b) Richardson, J. W., Jr.; Pluth, J. J.; Smith, J. V. *Acta Crystallogr.* **1988**, *B44*, 367.

(12) (a) Tapp, N. J.; Milestone, N. B.; Bibby, D. M. *Zeolites* **1988**, *8*, 183. (b) Ren, X.; Komarneni, S.; Roy, D. M. *Zeolites* **1991**, *11*, 142.

(13) a) Barrie, P. J.; Smith, M. E.; Klinowski, J. *Chem. Phys. Lett.* **1991**, *180*, 6. (b) Peeters, M. P. J.; de Hann, J. W.; van de Ven, L. J.; van Hooff, J. H. C. *J. Phys. Chem.* **1993**, *97*, 5363.

(14) (a) Fernandez, C.; Delevoye, L.; Amoureux, J.-P.; Pruski, M. *J. Am. Chem. Soc.* **1997**, *119*, 6858. (b) Fernandez, C.; Amoureux, J.-P. *Chem. Phys. Lett.* **1995**, *242*, 449.

(15) Khouzami, R.; Coudurier, G.; Lefebvre, F.; Vedrine, J. C., Mentzen, B. F. *Zeolites* **1990**, *10*, 183.

(16) Vega, A. J. *Solid State NMR* **1992**, *1*, 17.

(17) Amoureux, J.-P.; Fernandez, C.; Steuernagel, S. *J. Magn. Reson.* **1996**, *A13*, 116.

(18) (a) Sayari, A.; Moudrakovski, I.; Reddy, J. S.; Ratcliffe, C. I.; Ripmeester, J. A.; Preston, K. F. *Chem. Mater.* **1996**, *8*, 2080. (b) Blackwell, C. S.; Patton, R. L. *J. Phys. Chem.* **1988**, *92*, 3965. (c) Hasha, D.; Saldarriaga, L.; Hathaway, P. E.; Cox, D. F.; Davis, M. E. *J. Am. Chem. Soc.* **1988**, *110*, 2127.

(19) (a) Davis, M. E.; Monte, C.; Hathaway, P. E.; Grace, J. M. In *Zeolites: Facts, Figures, Future*; Jacobs, P. A., van Santen, R. A., Eds.; Elsevier: Amsterdam, 1989; pp 199−215. (b) He, H.; Klinowski, J. *J. Phys. Chem.* **1994**, *98* 1192. (c) Prasad, S.; Liu, S. B. *Chem. Mater.* **1994**, *6*, 633. (d) Liu, Z.; Xu, W.; Yang, G.; Xu, R. *Micropor. Mesopor. Mater.* **1998**, *22*, 33. (e) Akolekar, Bhargava, S. K.; Gorman, J.; Paterson, P. *Colloids and Surfaces*, **1999**, *146*, 375. (f) Jahn, E.; Mueller, D.; Richter-Mendau, J. In *Synthesis of Microporous Materials*; Occelli, M. L., Robson, H. E., Eds.; Van Nostrand Reinhold: New York, 1992; Vol. I, p 249.

(20) (a) Mortlock, R. F.; Bell, A. T.; Radke, C. J. *J. Phys. Chem.* **1993**, *97*, 767. (b) Mortlock, R. F.; Bell, A. T.; Radke, C. J. *J. Phys. Chem.* **1993**, *97*, 775.

(21) (a) Hartmann, P.; Vogel, J.; Schnabel, B. J. *Magn. Reson.* **1994**, *111*, 110. (b) Grimmer, A.-R.; Haubenreisser, U. *Chem. Phys. Lett.* **1983**, *99*, 487. (c) Mudrakovskii, I. L.; Shmachkova, V. P.; Kotsarenko, N. S.; Mastikhin, V. M. *J. Phys. Chem. Solids* **1986**, *47*, 335.

(22) (a) Burkett, S. L.; Davis, M. E. *J. Phys. Chem.* **1994**, *98*, 4647. (b) Gittleman, C. S.; Watanabe, K.; Bell, A. T.; Radke, C. J. *Micropor. Mater.* **1996**, *6*, 131.

(23) (a) Shantz, D. F.; Lobo, R. F. *J. Phys. Chem.* **1999**, *103*, 5920. (b) Shantz, D. F.; Lobo, R. F. *J. Am. Chem. Soc.* **1998**, *120*, 2482.

(24) (a) Vega, A. J. *J. Am. Chem. Soc.* **1988**, *110*, 1049. (b) Fyfe, C. A.; Zhang, Y.; Aroca, P. *J. Am. Chem. Soc.* **1992**, *114*, 3252.

(25) Fyfe, C. A.; Woon-Moon, K. C.; Huang, Y.; Grondey, H.; Mueller, K. T. *J. Phys. Chem.* **1995**, *99*, 8707.

(26) Vega, A. J. *J. Magn. Reson*. **1992**, *96*, 50.

(27) De Paul, S. M.; Ernst, M.; Shore, J. S.; Stebbins, J. F.; Pines, A. *J. Phys. Chem. B* **1997**, *101*, 3240.

(28) van Eck, E. R. H.; Kentgens, A. P. M.; Kraus, H.; Prins, R. *J. Phys. Chem.* **1995**, *99*, 16080.

(29) Dufau, N.; Lucian, L.; Rouquerol, F.; Llwewllyn, P. *J. Mater. Chem.* **2001**, *11*, 1300.

(30) For reviews, see: (a) Ortin, N. J.; Kruger, T. A.; Dutta, P. K. in *Analytical Applications of Raman Spectroscopy*; Pelletier, M. J., Ed.; Blackwell Science: Oxford, 1999; p 328. (b) Dutta, P. K. *J. Inclusion Phenom. Mol. Recognit. Chem.* **1995**, *21*, 215.

(31) Holmes, A. J.; Kirby, S. J.; Ozin, G. A.; Young, D. *J. Phys. Chem.* **1994**, *98*, 4677.